Eur. Phys. J. Spec. Top. (2026) 235:7989–7999
https://doi.org/10.1140/epjs/s11734-026-02481-x

THE EUROPEAN PHYSICAL JOURNAL SPECIAL TOPICS

Regular Article

Frequency-specific alterations of functional brain network measures in stereo-EEG recordings of epilepsy patients

Alexander Kuc[1,a], Andrey Zuev[2,b], Nikita Utashev[2,c], and Oleg Karpov[2,d]

[1] Research Institute of Applied Artificial Intelligence and Digital Solutions, Plekhanov Russian University of Economics, 36 Stremyannyy Pereulok, Moscow 115054, Russia
[2] Pirogov National Medical and Surgical Center, 70 Nizhnyaya Pervomayskaya Street, Moscow 105203, Russia

Received 30 May 2026 / Accepted 19 June 2026 / Published online 3 July 2026
© The Author(s), under exclusive licence to EDP Sciences, Springer-Verlag GmbH Germany, part of Springer Nature 2026

Abstract Epilepsy is increasingly considered a disorder of large-scale brain network organization characterized by abnormal interactions between distributed neuronal populations. In the present study, we investigated frequency-specific alterations of functional brain network topology in patients with focal epilepsy using graph-theoretical analysis of stereo-electroencephalography (sEEG) recordings. Functional connectivity networks were reconstructed using imaginary coherence within delta, theta, alpha, beta, low-gamma, and high-gamma frequency bands. Network topology was characterized using node strength, clustering coefficient, and participation coefficient. Comparative analysis between epileptogenic zones (EZ) and non-epileptic zones (non-EZ) revealed significant frequency-dependent differences in functional network organization. In particular, EZ channels demonstrated increased node strength in beta and gamma frequency bands, indicating enhanced global functional integration, while clustering coefficient was significantly reduced in beta and gamma networks, suggesting decreased local segregation and altered local connectivity organization. Participation coefficient analysis additionally revealed changes in intermodular interactions. The strongest alterations were observed within beta and high-gamma activity, emphasizing the important role of high-frequency oscillatory interactions in epileptogenic network dynamics. The obtained results support the concept of epilepsy as a network disorder involving large-scale reorganization of functional interactions rather than isolated local abnormalities and demonstrate the usefulness of graph-theoretical analysis for investigating pathological brain network organization.

1 Introduction

Epilepsy is one of the most common neurological disorders [1]. Traditionally, epilepsy was primarily considered a focal pathology associated with localized regions of abnormal neuronal excitability [2]. However, modern neurophysiological and neuroimaging studies increasingly support the concept of epilepsy as a disorder of large-scale brain networks, in which seizure generation and propagation emerge from abnormal interactions between distributed neuronal populations rather than isolated pathological foci alone [3].

Within the framework of network neuroscience, the brain can be represented as a complex system composed of interconnected functional and structural elements whose interactions determine large-scale neuronal dynamics [4]. Functional brain networks are typically reconstructed from statistical dependencies between neurophysiological signals and subsequently analyzed using graph-theoretical approaches. Such methods enable quantitative characterization of network topology, including network integration, segregation, modular organization, and hub structure [5]. Similar network-based approaches have been successfully applied to characterize functional reorganization in other brain disorders, including major depressive disorder [6, 7] and disorders of consciousness [8], highlighting common principles of network disruption across neurological conditions.

Over the last decade, graph-theoretical analysis has become an important tool for investigating pathological brain organization in epilepsy. Previous studies demonstrated that epileptic brain networks exhibit altered topological

[a] e-mail: kuc1995@mail.ru (corresponding author)
[b] e-mail: zuevaa@pirogov-center.ru
[c] e-mail: utyashevnp@pirogov-center.ru
[d] e-mail: info@pirogov-center.ru

properties compared to normal brain activity, including changes in clustering coefficient, path length, centrality, efficiency, and modular organization [9]. These alterations have been observed both during seizures and during interictal periods, suggesting that epilepsy is associated with persistent reorganization of functional interactions even outside seizure events [10].

Particular attention has been devoted to the investigation of epileptogenic zones (EZ), which are considered key regions involved in seizure initiation and propagation. Functional connectivity studies have demonstrated that EZ regions often exhibit abnormal synchronization patterns and altered connectivity strength relative to surrounding brain tissue [11]. Such findings support the hypothesis that epileptogenic regions may function as pathological network hubs characterized by enhanced participation in large-scale synchronization processes.

Stereo-electroencephalography (sEEG) provides unique opportunities for studying functional brain networks in epilepsy due to its high temporal resolution, high signal-to-noise ratio, and direct intracranial recording of neuronal activity [12]. In contrast to scalp EEG [13], sEEG enables investigation of functional interactions between deep brain structures with reduced influence of volume conduction and signal mixing [14]. As a result, sEEG-based functional connectivity analysis has become an important approach for characterizing epileptic network organization and identifying pathological brain interactions. Recent advances in seizure detection from intracranial recordings have leveraged extreme value theory and deep learning architectures [15, 16], demonstrating the potential of data-driven methods for analyzing epileptic brain activity.

Functional connectivity in sEEG recordings can be estimated using multiple synchronization measures, including coherence, phase-locking value, mutual information, and correlation-based metrics [17]. In the present study, we employed imaginary coherence (imcoh), which selectively captures non-zero phase–lag interactions and reduces the influence of spurious zero–lag correlations caused by common sources or volume conduction [18]. This measure is particularly suitable for intracranial EEG analysis and has been widely applied in studies of functional brain connectivity.

Recent studies suggest that epileptic activity is strongly frequency-dependent and involves distinct oscillatory mechanisms across different frequency bands [19]. In particular, beta and gamma oscillations are believed to play an important role in pathological synchronization, seizure propagation, and abnormal neuronal recruitment [20]. Therefore, frequency-specific analysis of functional network organization may provide important insights into the mechanisms underlying epileptic dynamics.

Despite substantial progress in network-based epilepsy research, the relationship between local and global topological alterations in epileptogenic networks remains insufficiently understood. In particular, relatively few studies have simultaneously investigated network integration, local segregation, and intermodular organization across multiple frequency bands using intracranial recordings.

In the present study, we investigate frequency-specific alterations of functional brain network topology in patients with focal epilepsy using graph-theoretical analysis of sEEG functional connectivity networks. Functional connectivity was reconstructed using imaginary coherence within multiple frequency bands, and the resulting networks were analyzed using node strength, clustering coefficient, and participation coefficient. We hypothesized that epileptogenic zones exhibit characteristic alterations of network topology reflecting abnormal functional organization and pathological synchronization processes.

The methodological and conceptual novelty of this work is threefold. First, unlike most prior sEEG studies that focused on a single frequency band or combined bands without systematic comparison, we perform a parallel, multi-band analysis (delta–high-gamma) within the same patient cohort, allowing direct comparison of frequency-dependent effects. Second, by simultaneously assessing integration (node strength), segregation (clustering coefficient), and intermodular connectivity (participation coefficient), we provide a more comprehensive characterization of network reorganization than studies relying on a single metric. Third, while previous graph-theoretical investigations often emphasized either global network changes or local EZ properties, our approach explicitly links local topological alterations in EZ channels to broader network-level reorganization, thus testing the hypothesis that epileptogenic regions function as pathological hubs with distinct frequency-specific signatures. This integrated perspective helps bridge the gap between focal and network-level conceptualizations of epilepsy.

The obtained results demonstrate significant frequency-dependent reorganization of epileptic functional networks, particularly within beta and gamma frequency ranges. Specifically, epileptogenic regions exhibited increased network integration together with reduced local segregation, supporting the concept of epilepsy as a disorder of large-scale functional brain interactions. This pattern of altered integration and segregation resembles that observed in other neuropsychiatric disorders [6], suggesting a transdiagnostic mechanism of network dysfunction.

2 Materials and methods

2.1 Stereo-EEG recordings

This study retrospectively included stereo-electroencephalography (sEEG) data from 18 patients with drug-resistant focal epilepsy treated at the N.I. Pirogov National Medical and Surgical Center. All participants gave their voluntary written informed consent.

The inclusion criteria for patients in the study were as follows: age of 18 years or older, confirmed focal drug-resistant epilepsy, undergone sEEG, availability of archived sEEG recordings, and the ability to assess the ictal pattern based on intracranial monitoring data.

All patients underwent prolonged invasive monitoring using depth electrodes. Implantation accuracy was verified by comparison with individual preoperative MRI images. For registration, semi-flexible platinum–iridium stereo-EEG electrodes with 6 to 16 contacts (contact length – 2 mm, diameter – 0.8 mm, intercontact distance – 1.5 mm) were used. Implantation was performed using a ROSA stereotactic robotic system under endotracheal anesthesia. SEEG signals were recorded using certified systems (XLTEK, Brain Quick, EB-neuro) with a sampling rate of 256 Hz, bandpass filtering of 0.15–100 Hz, and a 50 Hz notch filter. Subsequent processing included re-referencing to a bipolar montage by calculating the potential difference between adjacent contacts on the same electrode.

The seizure onset zone (SOZ) was identified by a clinically experienced epileptologist based on characteristic electrophysiological patterns during ictal onset [21, 22]. Importantly, surgical resection of this zone led to complete seizure freedom in all patients for at least 3 years postoperatively, providing robust clinical validation of the accuracy of SOZ localization. Although the surgically defined SOZ does not necessarily coincide with the absolute biological epileptogenic substrate [23], the favorable outcome in each patient confirms its validity for subsequent analysis.

It is important to clarify the distinction between the concepts of seizure onset zone (SOZ) and epileptogenic zone (EZ), as these terms are often used interchangeably in the clinical literature despite referring to related but non-identical constructs. The SOZ is defined operationally as the brain region, where the first unambiguous ictal discharge is observed at seizure onset, whereas the EZ represents the broader cortical network whose removal is both necessary and sufficient to achieve seizure freedom [24]. In practice, the SOZ is typically considered a reliable surrogate marker of the EZ, particularly when surgical resection of the SOZ results in favorable postoperative outcomes, as in the present cohort. Therefore, throughout this manuscript we use the abbreviation EZ to denote the channels belonging to the seizure onset zone, consistent with the common clinical convention that treats the SOZ as the observable manifestation of the underlying epileptogenic network. This terminology choice aligns with the network-oriented perspective of the study, which conceptualizes epilepsy as a disorder of distributed functional interactions rather than a purely focal abnormality.

2.2 Signal preprocessing

SEEG recordings were preprocessed and analyzed using the MNE–Python framework [25]. To investigate frequency-specific functional interactions, the recordings were filtered into several conventional frequency bands associated with different neuronal oscillatory processes: delta (1–4 Hz), theta (4–8 Hz), alpha (8–13 Hz), beta (13–30 Hz), low-gamma (30–60 Hz), high-gamma (60–100 Hz).

Bandpass filtering was performed independently for each frequency range using finite impulse response (FIR) filters.

For subsequent connectivity analysis, continuous sEEG recordings were segmented into overlapping temporal windows. Window duration was set to 2 s with 50% overlap between consecutive windows. The use of overlapping windows improved the stability of functional connectivity estimation while preserving the temporal variability of neuronal interactions.

2.3 Functional connectivity estimation

Functional connectivity between sEEG channels was estimated using imaginary coherence (ImCoh), a frequency-domain measure of phase synchronization that is less sensitive to the effects of volume conduction and common reference artifacts compared to conventional coherence measures [18].

For each pair of sEEG channels $x_i(t)$ and $x_j(t)$, the cross-spectral density was computed in the frequency domain. Let $S_{ij}(f)$ denote the cross-spectrum between signals i and j, while $S_{ii}(f)$ and $S_{jj}(f)$ represent the corresponding auto-spectral densities. The complex coherency between two signals is defined as

$$C_{ij}(f) = \frac{S_{ij}(f)}{\sqrt{S_{ii}(f)S_{jj}(f)}} \tag{1}$$

where $C_{ij}(f)$ is a complex-valued quantity characterizing the phase and amplitude consistency between signals at frequency f.

In the present study, functional connectivity was quantified using the imaginary part of coherency:

$$\mathrm{ImCoh}_{ij}(f) = |\mathrm{Im}(C_{ij}(f))| \tag{2}$$

The imaginary coherence measure selectively captures non-zero phase–lag interactions between signals and suppresses spurious correlations arising from instantaneous coupling or volume conduction. This property is particularly important for intracranial EEG analysis, where neighboring electrodes may exhibit artificially inflated zero–lag correlations due to common signal sources.

Connectivity estimation was performed independently within each predefined frequency band. For every temporal window, a connectivity matrix was constructed:

$$\mathbf{W} = [w_{ij}]_{N\times N} \tag{3}$$

where N denotes the number of sEEG channels and w_{ij} corresponds to the imaginary coherence value between channels i and j.

Connectivity matrices obtained from all temporal windows were subsequently averaged to obtain a single representative functional connectivity matrix for each recording and frequency band:

$$\bar{W}_{ij} = \frac{1}{K}\sum k = 1^{K} W_{ij}^{(k)} \tag{4}$$

where K is the number of temporal windows and $W_{ij}^{(k)}$ denotes the connectivity value for channels i and j in the kth window.

The resulting connectivity matrices were symmetrized to ensure undirected network representation:

$$W_{ij}^{sym} = \frac{W_{ij} + W_{ji}}{2} \tag{5}$$

Diagonal elements were set to zero in order to exclude self-connections from subsequent graph analysis.

The obtained weighted connectivity matrices represented functional brain networks in which sEEG channels corresponded to network nodes and imaginary coherence values represented weighted functional interactions between neuronal populations.

2.4 Network measures

Functional connectivity matrices were analyzed within the framework of graph theory in order to characterize the topological organization of functional brain networks. Each connectivity matrix was interpreted as a weighted undirected graph:

$$G = (V, E, W) \tag{6}$$

where V denotes the set of network nodes corresponding to sEEG channels, E represents the set of edges describing functional interactions between channels, and W is the weighted adjacency matrix containing imaginary coherence values.

To reduce the influence of weak and potentially noisy connections, graph measures characterizing network topology were computed after thresholding the connectivity matrices. Specifically, only the strongest 20% of functional connections were preserved. Let N denote the number of nodes in the network. The total number of possible undirected edges is given by

$$N_{\mathrm{edges}} = \frac{N(N-1)}{2} \tag{7}$$

A threshold corresponding to the top 20% of connectivity values was applied to construct sparse binary network representations while preserving the strongest functional interactions.

The choice of the 20% threshold was guided by several methodological considerations. This value represents a commonly adopted proportion in functional brain network studies using intracranial EEG, providing a balance between retaining sufficiently dense connectivity patterns for robust graph analysis and eliminating spurious or weak correlations that may arise from physiological noise or limited signal-to-noise ratio [26]. It should be noted that

threshold selection inherently influences absolute values of graph-theoretical metrics, such as clustering coefficient and participation coefficient, as the number of retained edges directly affects local connectivity density and modular structure detection. However, since the same threshold was applied consistently across all recordings, frequency bands, and anatomical groups, the relative comparisons between EZ and non-EZ conditions remain valid and interpretable. This approach follows the standard practice in the field, where thresholding is used to focus on the most functionally significant connections while acknowledging that absolute metric values may depend on the chosen sparsity level.

Three complementary graph-theoretical measures were analyzed: node strength, clustering coefficient, and participation coefficient. These metrics characterize different aspects of functional network organization including global integration, local segregation, and intermodular connectivity [26].

Node strength. Node strength quantifies the overall level of functional connectivity associated with a given node and serves as a measure of network integration. For node i, node strength was computed as

$$s_i = \sum_{j=1}^{N} w_{ij} \tag{8}$$

where w_{ij} denotes the weighted functional connection between nodes i and j.

Higher node strength values indicate stronger integration of a node into large-scale functional interactions and may reflect increased participation in synchronized neuronal activity.

Clustering coefficient. The clustering coefficient characterizes the tendency of neighboring nodes to form locally interconnected groups and, therefore, reflects local segregation of the network.

In the present study, a weighted clustering coefficient based on the formulation proposed by Onnela et al. was used [27]. For node i, the coefficient is defined as

$$C_i = \frac{1}{k_i(k_i-1)} \sum_{j,k} (w_{ij} w_{jk} w_{ki})^{1/3} \tag{9}$$

where k_i denotes the degree of node i, and the summation is performed over neighboring nodes forming triangular motifs.

The clustering coefficient reflects the density of local functional interactions surrounding a node. High values indicate strong local interconnectedness and increased local segregation within the network.

Participation coefficient. The participation coefficient characterizes the distribution of a node's connections across different network modules and, therefore, reflects intermodular connectivity organization.

Network modules were identified using the Louvain community detection algorithm [28]. The participation coefficient for node i was computed as

$$P_i = 1 - \sum_{m=1}^{M} \left(\frac{k_i(m)}{k_i} \right)^2 \tag{10}$$

where k_i denotes the total strength of node i, $k_i(m)$ is the strength of connections from node i to nodes belonging to module m, and M is the total number of detected modules.

High participation coefficient values indicate that a node interacts with multiple network modules and may, therefore, act as an integrative connector between different functional communities.

Together, the selected network measures provided complementary information about the organization of epileptic functional brain networks at both local and global scales.

2.5 Statistical analysis

Statistical analysis was performed to identify significant differences in functional network organization between epileptogenic zones (EZ) and non-epileptogenic zones (non-EZ) across different frequency bands.

For each recording and each frequency band, network measures were first computed independently for all sEEG channels. Subsequently, channels were separated into two groups according to clinical labeling: channels belonging to the epileptogenic zone and channels belonging to non-epileptogenic zones. To reduce the influence of local variability and unequal numbers of contacts across recordings, network measures were averaged within each group:

$$\bar{x}_{\mathrm{EZ}} = \frac{1}{N_{\mathrm{EZ}}} \sum_{i=1}^{N_{\mathrm{EZ}}} x_i \tag{11}$$

and

$$\bar{x}_{\text{non-EZ}} = \frac{1}{N_{\text{non-EZ}}} \sum_{i=1}^{N_{\text{non-EZ}}} x_i \tag{12}$$

where x_i denotes the network measure value for channel i, while N_{EZ} and $N_{\text{non-EZ}}$ represent the numbers of channels belonging to EZ and non-EZ, respectively.

This aggregation procedure yielded one representative value per recording, frequency band, and anatomical group for each network metric. Such an approach allowed controlling for inter-recording variability and ensured that statistical comparisons reflected differences between functional network organizations rather than differences in the number of channels.

Comparisons between EZ and non-EZ were performed independently for each frequency band and each network measure. Since EZ and non-EZ values originated from the same recording, paired statistical analysis was applied. Specifically, paired Student's t tests were used to evaluate statistical significance of differences between groups:

$$t = \frac{\bar{d}}{s_d/\sqrt{n}} \tag{13}$$

where $\bar{d}$ denotes the mean difference between paired observations, s_d is the standard deviation of paired differences, and n is the number of recordings included in the analysis.

To account for multiple statistical comparisons across frequency bands and network metrics, false discovery rate (FDR) correction using the Benjamini–Hochberg procedure was applied. Corrected p values were obtained according to

$$p_i^{FDR} = \frac{p_i m}{i} \tag{14}$$

where p_i denotes the ordered p value, i is its rank after sorting, and m represents the total number of performed comparisons.

Differences were considered statistically significant for corrected p values satisfying ($p_{\text{FDR}} < 0.05$).

For each comparison, the relative percentage difference between EZ and non-EZ was additionally computed as

$$\Delta(\%) = \frac{\bar{x}_{\text{EZ}} - \bar{x}_{\text{non-EZ}}}{\bar{x}_{\text{non-EZ}}} \times 100 \tag{15}$$

This measure enabled quantitative characterization of the magnitude and direction of network alterations in epileptogenic regions.

The statistical analysis pipeline, therefore, allowed systematic evaluation of frequency-specific differences in network topology between epileptogenic and non-involved brain regions while controlling for multiple comparisons and inter-recording variability.

3 Results

The comparative analysis between epileptogenic zones and non-epileptogenic zones revealed pronounced frequency-specific differences in functional network organization across several graph-theoretical measures. The obtained statistical analysis results are shown in Table 1, and also summarized in Fig. 1, which presents the relative percentage differences between EZ and non-EZ for all analyzed frequency bands and network metrics. Positive values correspond to higher metric values within EZ channels, whereas negative values indicate reduced values relative to non-EZ. Statistical significance after FDR correction is indicated by asterisks.

The most prominent alterations were observed in beta and gamma frequency ranges. In particular, node strength demonstrated significant increases in EZ channels within the beta and high-gamma bands. The strongest effect was observed in the beta band, where EZ channels exhibited an 18.2% increase in node strength compared to non-EZ channels ($p_{\text{FDR}} = 3 \times 10^{-6}$). Similarly, high-gamma networks demonstrated a 12.8% increase in strength within EZ ($p_{\text{FDR}} = 5.5 \times 10^{-5}$), while low-gamma activity showed a smaller but still significant increase of 9.9% ($p_{\text{FDR}} = 8.8 \times 10^{-3}$).

These results indicate enhanced functional integration of epileptogenic regions into large-scale functional brain interactions, particularly in high-frequency oscillatory activity. In contrast, theta-band networks demonstrated an

Table 1 Comparison of network metrics between EZ and non-EZ zones

Band	Metric	p value	p (FDR)	Sig.
Delta	Strength	1.15e−01	1.59e−01	–
Delta	Clustering coefficient	8.89e−01	8.89e−01	–
Delta	Participation coefficient	3.51e−01	4.21e−01	–
Theta	Strength	8.11e−05	3.65e−04	*
Theta	Clustering coefficient	7.23e−03	1.45e−02	*
Theta	Participation coefficient	4.80e−03	1.08e−02	*
Alpha	Strength	1.41e−01	1.82e−01	–
Alpha	Clustering coefficient	4.61e−02	6.91e−02	–
Alpha	Participation coefficient	7.31e−01	7.74e−01	–
Beta	Strength	2.86e−07	3.00e−06	*
Beta	Clustering coefficient	4.25e−04	1.53e−03	*
Beta	Participation coefficient	8.90e−03	1.60e−02	*
Low gamma	Strength	3.43e−03	8.81e−03	*
Low gamma	Clustering coefficient	2.97e−03	8.81e−03	*
Low gamma	Participation coefficient	2.75e−02	4.50e−02	*
High gamma	Strength	9.18e−06	5.50e−05	*
High gamma	Clustering coefficient	8.93e−08	2.00e−06	*
High gamma	Participation coefficient	3.84e−01	4.32e−01	–

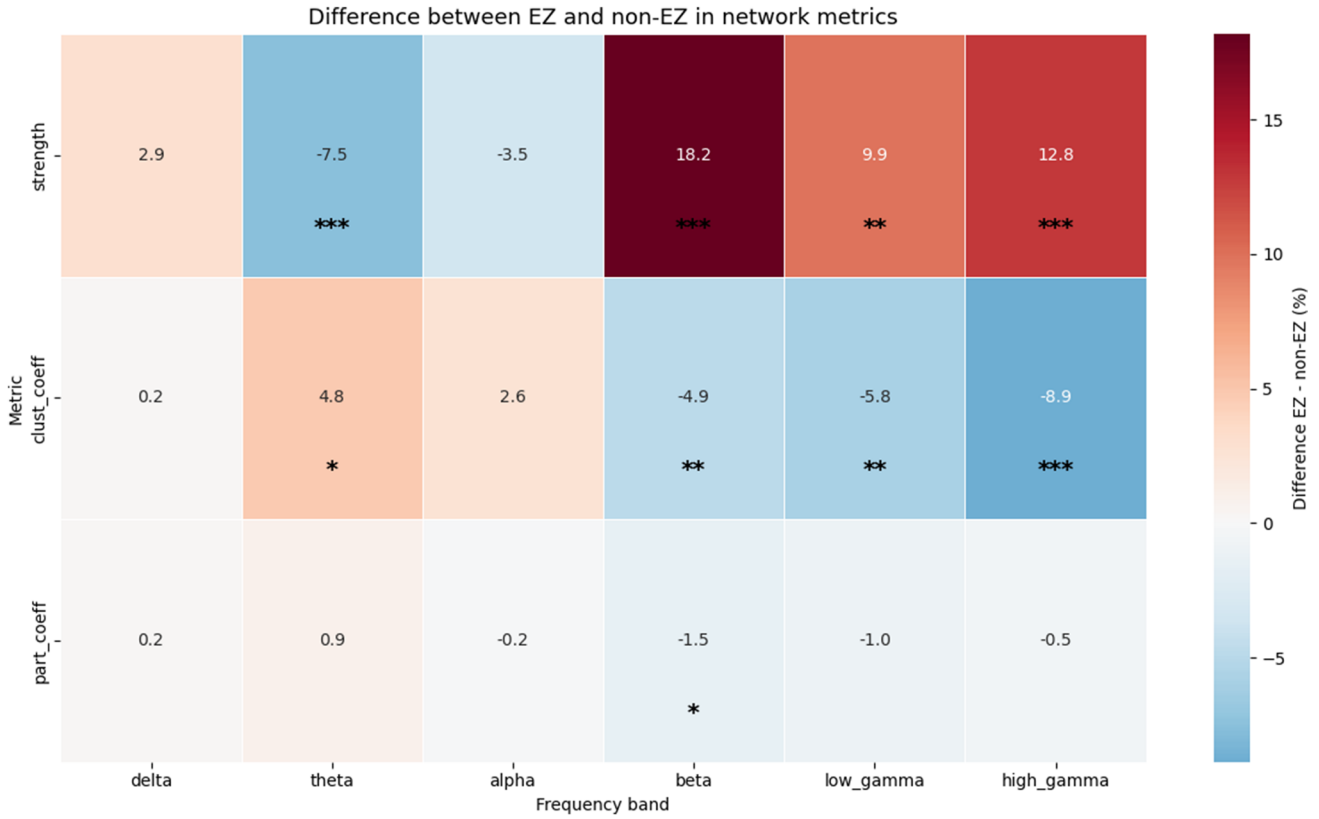


Fig. 1 Percentage differences in network metric values between EZ and non-EZ across different frequency bands. Positive values indicate higher metric values in EZ, negative values indicate lower values. *$p_{\mathrm{FDR}} < 0.05$

opposite tendency, with EZ channels exhibiting significantly lower node strength compared to non-EZ channels (-7.5%, $p_{\mathrm{FDR}} = 3.7 \times 10^{-4}$).

Substantial differences were also observed for clustering coefficient, which characterizes local segregation and local interconnectedness of the network. The strongest reduction was identified in the high-gamma band, where clustering coefficient decreased by 8.9% in EZ channels relative to non-EZ ($p_{\mathrm{FDR}} = 2\times10^{-6}$). Significant reductions were additionally observed in the low gamma (-5.8%, $p_{\mathrm{FDR}} = 8.8 \times 10^{-3}$) and beta ($-4.9\%$, $p_{\mathrm{FDR}} = 1.5 \times 10^{-3}$) frequency bands.

These findings suggest that epileptogenic regions are characterized not only by stronger global integration but also by reduced local segregation, indicating substantial reorganization of local functional interactions within pathological brain networks.

Unlike gamma and beta bands, theta-band activity demonstrated an increase in clustering coefficient within EZ channels ($+4.8\%$, $p_{\mathrm{FDR}} = 1.6 \times 10^{-2}$). This result may reflect frequency-dependent differences in network organization mechanisms underlying epileptic activity.

Participation coefficient analysis revealed weaker but still statistically significant alterations in intermodular connectivity organization. In the theta band, EZ channels demonstrated a slight increase in participation coefficient ($+1.16\%$, $p_{\mathrm{FDR}} = 2.0 \times 10^{-2}$), suggesting enhanced interactions between different functional modules. Conversely, beta-band networks exhibited reduced participation coefficient within EZ (-1.31%, $p_{\mathrm{FDR}} = 4.6\times10^{-2}$), potentially indicating partial isolation or restructuring of functional communities in epileptogenic regions.

Overall, the obtained results demonstrate that epileptogenic zones exhibit substantial frequency-dependent reorganization of functional network topology, with the strongest effects consistently localized within beta and gamma oscillatory activity.

4 Discussion

The present study investigated frequency-specific alterations of functional brain network topology in patients with focal epilepsy using graph-theoretical analysis of sEEG functional connectivity networks. The obtained results demonstrated significant differences between epileptogenic zones and non-epileptogenic zones, particularly within beta and gamma frequency bands. The observed effects included increased node strength together with reduced clustering coefficients in epileptogenic regions, indicating large-scale reorganization of pathological brain interactions.

One of the most prominent findings of the study was the significant increase in node strength within EZ channels in beta and gamma frequency bands. The strongest effect was observed in the beta band, where node strength increased by more than 18% relative to non-EZ channels. Similar increases were also identified in low-gamma and high-gamma activity. Since node strength reflects the total level of functional connectivity associated with a given node, these findings suggest enhanced integration of epileptogenic regions into large-scale functional interactions.

Such increased integration may reflect abnormal synchronization processes facilitating seizure generation and propagation [29]. Previous studies have demonstrated that epileptic activity is associated with excessive synchronization and increased functional coupling between neuronal populations [30]. Within the framework of network neuroscience, epileptogenic regions may, therefore, act as highly integrated network hubs participating in pathological information exchange and synchronization dynamics [31]. This pattern of increased global integration with reduced local segregation is consistent with findings in major depressive disorder, where disrupted segregation mechanisms in functional brain networks have been linked to symptom severity [6, 7].

At the same time, clustering coefficient demonstrated significant reductions in beta and gamma frequency bands, with the strongest decrease observed in high-gamma activity. Since clustering coefficient reflects the density of local interconnections between neighboring nodes, reduced clustering suggests disruption of local network segregation and weakening of locally organized functional interactions.

The simultaneous increase in node strength and decrease in clustering coefficient is particularly important for interpreting the organization of epileptogenic networks. Such a combination indicates that epileptogenic regions become more globally integrated while losing local topological specialization [32]. In other words, pathological networks appear to shift toward more distributed large-scale synchronization patterns accompanied by reduced local modular organization.

This interpretation is consistent with the modern concept of epilepsy as a disorder of large-scale brain network organization rather than a purely focal pathology. From this perspective, epileptogenic zones should not be considered isolated generators of pathological activity but rather central components of distributed functional networks supporting seizure dynamics [33].

The strongest alterations observed in beta and gamma frequency bands may reflect the specific role of high-frequency oscillatory activity in epileptic dynamics. Gamma oscillations are closely associated with local neuronal synchronization, excitation–inhibition balance, and pathological hypersynchronous activity [20]. Increased high-frequency connectivity within EZ may, therefore, indicate enhanced recruitment of neuronal populations into

synchronized pathological activity. Similar frequency-specific alterations have been observed in other brain disorders; for instance, patients with disorders of consciousness show multiscale network disruptions across different frequency bands [8].

Interestingly, theta-band activity demonstrated partially opposite tendencies compared to beta and gamma networks. In particular, EZ channels exhibited reduced node strength together with increased clustering coefficient and participation coefficient. These results suggest that low-frequency functional interactions may involve different organizational mechanisms compared to high-frequency epileptic synchronization.

One possible interpretation is that theta-band activity reflects compensatory or regulatory network processes rather than direct pathological synchronization. Increased clustering in theta networks may indicate preservation or reinforcement of local interactions, whereas reduced strength may reflect weaker long-range synchronization relative to high-frequency epileptic activity [34]. However, the precise physiological interpretation of these frequency-dependent effects requires further investigation.

Participation coefficient analysis revealed comparatively weaker differences between EZ and non-EZ. Nevertheless, significant alterations in theta and beta bands indicate partial reorganization of intermodular connectivity patterns in epileptogenic networks. Reduced participation coefficient in the beta band may suggest that epileptogenic regions become more internally integrated while simultaneously exhibiting reduced interactions with other functional modules [35].

Importantly, the observed effects remained statistically significant after correction for multiple comparisons despite substantial inter-recording variability and heterogeneity of electrode implantation schemes. This suggests that the identified network alterations represent robust features of epileptogenic functional organization rather than recording-specific effects.

Several methodological aspects should also be considered when interpreting the results. First, functional connectivity estimation was based on imaginary coherence, which selectively captures non-zero phase–lag interactions and reduces the influence of volume conduction and common reference artifacts. This property is particularly important in intracranial EEG analysis, where neighboring electrodes may exhibit artificially elevated zero–lag correlations.

Second, graph analysis was performed using thresholded sparse networks preserving the strongest functional connections. Although threshold selection may influence absolute metric values, the applied approach enabled stable comparison of relative topological differences between EZ and non-EZ across recordings.

The present study has several limitations. The analyzed patient cohort included recordings with heterogeneous implantation schemes and different epileptic localizations. Furthermore, the analysis was performed on interictal recordings and, therefore, reflects background pathological network organization rather than seizure dynamics themselves. Future studies may extend the proposed framework toward dynamic network analysis during seizure evolution and investigate temporal transitions between functional brain states.

Another important limitation concerns the relatively modest sample size of 18 patients included in this study. Future studies with larger, more homogeneous patient groups are needed to confirm the reproducibility of these findings and to investigate potential subgroup differences based on epilepsy type, localization, or etiology. In addition, larger cohorts would enable more sophisticated statistical modeling approaches, such as mixed-effects models or machine learning-based classification, which could further elucidate the relationship between network topology and clinical outcomes.

Future studies may extend the proposed framework toward dynamic network analysis during seizure evolution and investigate temporal transitions between functional brain states.

Another important direction for future work involves combining graph-theoretical analysis with more advanced approaches from higher-order network theory and topological data analysis [36, 37]. Such methods may provide additional information about mesoscale organization and collective interaction patterns in epileptic brain networks. Moreover, the integration of interpretable machine learning techniques [38, 39] could enhance the clinical utility of network-based biomarkers for localizing epileptogenic zones.

Overall, the obtained results support the concept that epilepsy is associated with frequency-specific reorganization of functional brain network topology [40]. The combination of enhanced global integration and reduced local segregation observed in epileptogenic regions suggests that pathological synchronization emerges through large-scale restructuring of functional interactions rather than isolated local abnormalities alone.

5 Conclusions

In the present study, we investigated frequency-specific alterations of functional brain network topology in patients with focal epilepsy using graph-theoretical analysis of sEEG functional connectivity networks. The obtained results demonstrated significant differences between epileptogenic zones and non-involved brain regions, particularly within beta and gamma frequency bands.

Epileptogenic regions were characterized by increased node strength together with reduced clustering coefficient, indicating enhanced global integration combined with decreased local segregation of functional interactions. These findings support the concept of epilepsy as a disorder of large-scale brain network organization rather than purely localized pathological activity.

The observed frequency-dependent alterations suggest that high-frequency oscillatory interactions play a key role in epileptogenic network dynamics. Overall, the proposed framework based on sEEG functional connectivity and graph-theoretical analysis provides an effective approach for investigating pathological brain interactions and may contribute to improved characterization of epileptogenic networks.

Acknowledgements This work is supported from the Russian Science Foundation (project 23-71-30010).

Data availability statement The data presented in this study are available on request from the corresponding author.

References

1. K.M. Fiest, K.M. Sauro, S. Wiebe, S.B. Patten, C.S. Kwon, J. Dykeman et al., Prevalence and incidence of epilepsy: a systematic review and meta-analysis of international studies. Neurology **88**(3), 296–303 (2017)
2. S. Shorvon, The evolution of epilepsy theory and practice at the national hospital for the relief and cure of epilepsy, queen square between 1860 and 1910. Epilepsy Behav. **31**, 228–242 (2014)
3. T. Bröhl, T. Rings, J. Pukropski, R. von Wrede, K. Lehnertz, The time-evolving epileptic brain network: concepts, definitions, accomplishments, perspectives. Front. Netw. Physiol. **3**, 1338864 (2024)
4. E. Bullmore, O. Sporns, Complex brain networks: graph theoretical analysis of structural and functional systems. Nat. Rev. Neurosci. **10**(3), 186–198 (2009)
5. J.R. Cohen, M. D'Esposito, The segregation and integration of distinct brain networks and their relationship to cognition. J. Neurosci. **36**(48), 12083–12094 (2016)
6. V.S. Khorev, S.A. Kurkin, G. Zlateva, R. Paunova, S. Kandilarova, M. Maes et al., Disruptions in segregation mechanisms in FMRI-based brain functional network predict the major depressive disorder condition. Chaos, Solitons Fractals **188**, 115566 (2024)
7. D. Stoyanov, V. Khorev, R. Paunova, S. Kandilarova, D. Simeonova, A. Badarin et al., Resting-state functional connectivity impairment in patients with major depressive episode. Int. J. Environ. Res. Public Health **19**(21), 14045 (2022)
8. S. Kurkin, L. Mayorova, V. Khorev, E. Pitsik, M. Radutnaya, E. Bondar et al., Multiscale FMRI analysis reveals hierarchical network disruptions underlying disorders of consciousness. Chaos, Solitons Fractals **200**, 117008 (2025)
9. E. Van Diessen, W.J. Zweiphenning, F.E. Jansen, C.J. Stam, K.P. Braun, W.M. Otte, Brain network organization in focal epilepsy: a systematic review and meta-analysis. PLoS ONE **9**(12), e114606 (2014)
10. A.N. Khambhati, D.S. Bassett, B.S. Oommen, S.H. Chen, T.H. Lucas, K.A. Davis et al., Recurring functional interactions predict network architecture of interictal and ictal states in neocortical epilepsy. Eneuro **4**(1), ENEURO.0091-16.2017 (2017)
11. Y. Wei, W. Zhang, S.X. Liu, B. Han, Q. Chen, Reproducibility of temporally evolving seizure patterns and network connectivity in focal epilepsy. Front. Neurol. **16**, 1617317 (2025)
12. S. Pati, S. Agashe, A. Kheder, K. Riley, J. Gavvala, R. McGovern et al., Stereoelectroencephalography of the deep brain: basal ganglia and thalami. J. Clin. Neurophysiol. **41**(5), 423–429 (2024)
13. V.V. Grubov, A.K. Kuc, S.A. Kurkin, D.A. Andrikov, N. Utyashev, V.A. Maksimenko et al., Harnessing long-range temporal correlations for advanced epilepsy classification. PRX Life **3**(1), 013005 (2025)
14. F. Bartolomei, S. Lagarde, F. Wendling, A. McGonigal, V. Jirsa, M. Guye et al., Defining epileptogenic networks: contribution of SEEG and signal analysis. Epilepsia **58**(7), 1131–1147 (2017)
15. O. Karpov, V. Grubov, V. Maksimenko, S. Kurkin, N. Smirnov, N. Utyashev et al., Extreme value theory inspires explainable machine learning approach for seizure detection. Sci. Rep. **12**(1), 11474 (2022)
16. V. Grubov, S. Nazarikov, S. Kurkin, N. Utyashev, D. Andrikov, O. Karpov et al., Two-stage approach with combination of outlier detection method and deep learning enhances automatic epileptic seizure detection. IEEE Access **12**, 122168–122182 (2024)
17. A.M. Bastos, J.M. Schoffelen, A tutorial review of functional connectivity analysis methods and their interpretational pitfalls. Front. Syst. Neurosci. **9**, 175 (2016)
18. G. Nolte, O. Bai, L. Wheaton, Z. Mari, S. Vorbach, M. Hallett, Identifying true brain interaction from EEG data using the imaginary part of coherency. Clin. Neurophysiol. **115**(10), 2292–2307 (2004)
19. G. Goelman, Z. Israel, S. Heymann, D. Ekstein, T. Benoliel, Exploratory analysis of epileptic and non-epileptiform hippocampal network organization across spatial and frequency domains. NeuroImage. **326**, 121698 (2026)
20. A. Medvedev, Temporal binding at gamma frequencies in the brain: paving the way to epilepsy? Australas. Phys. Eng. Sci. Med. **24**(1), 37–48 (2001)

21. P. Perucca, F. Dubeau, J. Gotman, Intracranial electroencephalographic seizure-onset patterns: effect of underlying pathology. Brain **137**(1), 183–196 (2014)
22. S. Lagarde, S. Buzori, A. Trebuchon, R. Carron, D. Scavarda, M. Milh et al., The repertoire of seizure onset patterns in human focal epilepsies: determinants and prognostic values. Epilepsia **60**(1), 85–95 (2019)
23. V. Jirsa, H. Wang, P. Triebkorn, M. Hashemi, J. Jha, J. Gonzalez-Martinez et al., Personalised virtual brain models in epilepsy. Lancet Neurol. **22**(5), 443–454 (2023)
24. A. Thomschewski, A.S. Hincapié, B. Frauscher, Localization of the epileptogenic zone using high frequency oscillations. Front. Neurol. **10**, 94 (2019)
25. A. Gramfort, M. Luessi, E. Larson, D.A. Engemann, D. Strohmeier, C. Brodbeck et al., MEG and EEG data analysis with MNE-Python. Front. Neurosci. **7**(267), 1–13 (2013). https://doi.org/10.3389/fnins.2013.00267
26. M. Rubinov, O. Sporns, Complex network measures of brain connectivity: uses and interpretations. Neuroimage **52**(3), 1059–1069 (2010)
27. J.P. Onnela, J. Saramäki, J. Kertész, K. Kaski, Intensity and coherence of motifs in weighted complex networks. Phys. Rev. E-Stat. Nonlinear Soft Matter Phys. **71**(6), 065103 (2005)
28. J. Zhang, J. Fei, X. Song, J. Feng, An improved Louvain algorithm for community detection. Math. Probl. Eng. **1**, 1485592 (2021)
29. P. Jiruska, M. De Curtis, J.G. Jefferys, C.A. Schevon, S.J. Schiff, K. Schindler, Synchronization and desynchronization in epilepsy: controversies and hypotheses. J. Physiol. **591**(4), 787–797 (2013)
30. C. Diaz Verdugo, S. Myren-Svelstad, E. Aydin, E. Van Hoeymissen, C. Deneubourg, S. Vanderhaeghe et al., Glia-neuron interactions underlie state transitions to generalized seizures. Nat. Commun. **10**(1), 3830 (2019)
31. C. Garcia-Ramos, J. Song, B. Hermann, V. Prabhakaran, Low functional robustness in mesial temporal lobe epilepsy. Epilepsy Res. **123**, 20–28 (2016)
32. S. Chiang, Z. Haneef, Graph theory findings in the pathophysiology of temporal lobe epilepsy. Clin. Neurophysiol. **125**(7), 1295–1305 (2014)
33. S.S. Spencer, Neural networks in human epilepsy: evidence of and implications for treatment. Epilepsia (Series 4) **43**(3), 219–227 (2002)
34. L. Douw, E. van Dellen, M. de Groot, J.J. Heimans, M. Klein, C.J. Stam et al., Epilepsy is related to theta band brain connectivity and network topology in brain tumor patients. BMC Neurosci. **11**(1), 103 (2010)
35. A. Lucas, E.J. Cornblath, N. Sinha, P. Hadar, L. Caciagli, S.S. Keller et al., Resting state functional connectivity demonstrates increased segregation in bilateral temporal lobe epilepsy. Epilepsia **64**(5), 1305–1317 (2023)
36. S.A. Kurkin, N.M. Smirnov, R. Paunova, S. Kandilarova, D. Stoyanov, L. Mayorova et al., Beyond pairwise interactions: higher-order q-analysis of FMRI-based brain functional networks in patients with major depressive disorder. IEEE Access **12**, 197168–197186 (2024)
37. S.A. Kurkin, A.N. Pisarchik, L.A. Mayorova, A.E. Hramov, Evolution of methods for assessing FMRI-based functional networks: from classical pairwise connectivity to higher-order interactions. Phys. Rep. **1174**, 1–66 (2026)
38. A.V. Andreev, S.A. Kurkin, D. Stoyanov, A.A. Badarin, R. Paunova, A.E. Hramov, Toward interpretability of machine learning methods for the classification of patients with major depressive disorder based on functional network measures. Chaos Interdiscipl. J. Nonlinear Sci. **33**(6) (2023)
39. M. Kabir, S. Kurkin, R. Paunova, D. Stoyanov, A. Hramov, Disentangling high-dimensional functional brain network structure in major depression via cortically inspired sparse encoding and contrastive learning. Chaos, Solitons Fractals **208**, 118234 (2024)
40. S. Chiang, A. Cassese, M. Guindani, M. Vannucci, H.J. Yeh, Z. Haneef et al., Time-dependence of graph theory metrics in functional connectivity analysis. Neuroimage **125**, 601–615 (2016)

Springer Nature or its licensor (e.g. a society or other partner) holds exclusive rights to this article under a publishing agreement with the author(s) or other rightsholder(s); author self-archiving of the accepted manuscript version of this article is solely governed by the terms of such publishing agreement and applicable law.